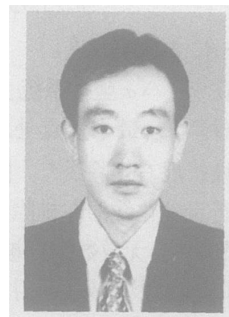


# 金属爆炸焊接界面应力场数值计算分析

谢飞鸿<sup>1,2</sup>, 罗冠炜<sup>3</sup>, 廖军生<sup>3</sup>, 汪旭光<sup>4</sup>

(1. 兰州交通大学 土木工程学院, 兰州 730070; 2. 北京科技大学 木与环境工程学院, 北京 100083; 3. 兰州交通大学 机电工程学院, 兰州 730070; 4. 北京矿冶研究总院, 北京 100044)



谢飞鸿

摘 要: 金属爆炸焊接材料的基、复板在炸药爆轰作用下产生的碰撞力是基、复板实现爆炸焊的关键条件。采用瑞利—里兹法计算模型, 根据弹性力学的变分原理, 将弹性力学问题表述为泛函驻值问题, 使泛函驻值的条件对应于所解问题的基本方程和边界条件, 从而推导出微分方程及对应的边界条件。计算碰撞点处的瞬时应力场, 同时对不同的碰撞角和碰撞压力进行了模拟计算, 发现了碰撞点处的应力场分布的基本规律。其应力场分布规律完全可以用于评价和指导实际的工程实践。

关键词: 爆炸焊接; 计算模型; 碰撞压力; 应力场; 数值计算

中图分类号: TG444 文献标识码: A 文章编号: 0253-360X(2006)10-026-03

## 0 序 言

金属材料的爆炸加工, 主要是依靠炸药的爆轰作用来驱动复板撞击基板材料, 在基复板材料接触面上产生高温、高压而实现材料的有效粘合(焊接), 研究压应力场在基或复板中的分布情况, 将有利于评价爆炸焊接的可靠性及焊接界面所发生的过熔或焊接程度。对于实际的爆炸焊接试件的有效加工, 选择合理的爆炸能量, 对碰撞压力是十分必要的, 利用弹性力学的变分原理, 将弹性力学问题表述为泛函驻值问题, 使泛函驻值的条件对应于所解问题的基本方程和边界条件, 从而推导出微分方程及对应的边界条件。由于变分法是以能量概念为基础的, 并从弹性体的总体上考虑问题, 因而更适合于文中所提出的问题。因此, 该计算模型所进行的数值分析, 将能够指导工程实践并为工程实践提供参考依据。

十万个大气压, 它将大大超过金属板材本身的动态屈服强度。由于其碰撞的压力为金属板材静态强度的几十倍甚至上百倍, 因此材料强度在该区域内是一个相对小量, 其碰撞速度可以达到每秒数公里, 厚度为基、复板 2%~5% 左右。它的形成意味着从两块相互复合(或焊接)的金属板材的内表面上剥掉一层包含氧化膜污染物的金属表面层, 使金属露出具有活性的清洁表面, 为两块金属板的焊接提供极为重要的条件。

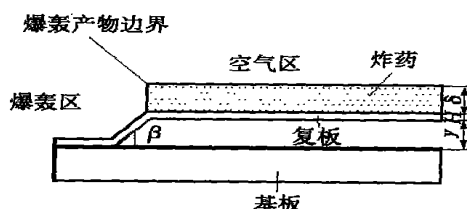


图 1 爆炸焊接加工形态图

Fig. 1 Appearance process of explosive welding

## 1 试件与模型

当炸药一端被引爆后, 见图<sup>[1~3]</sup>, 复板表面将迅速掠过一个高压冲击加载的“滑移爆轰波”, 复板在爆炸物的高压作用下迅速弯折, 在数毫秒的时间内, 复板被加速到每秒几百米的速度, 然后与基板相碰, 这个碰撞点将以每秒几公里的速度, 从引爆端开始, 依次掠过基板表面。其碰撞点的压力可达到几

将图 1 简化为图 2 的计算模型, 也就是将基板受复板冲击引起的应力、应变和位移按平面薄板弯曲问题进行求解。

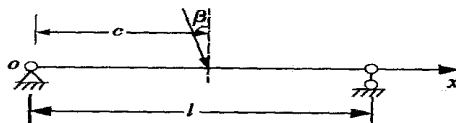


图 2 力学计算模型

Fig. 2 Mechanics computation model

## 2 数值计算与分析

### 2.1 瑞利—里兹(Rayleigh—Ritz)变分方程的直接解法计算模型<sup>[4]</sup>

考虑描述最小势能原理的位移变分方程  $\delta \Pi = 0$ ,  $\Pi$  称为总势能, 它是应变分量和位移分量的泛函, 设已知位移  $u_{0i}$  满足被考虑问题的位移边界条件, 已知函数  $u_{mi}$  ( $m = 1, 2, \dots, n$ ) 在边界上的值为零,  $m$  为振型阶数, 则可能位移便可表示为

$$u_i = u_{0i} + \sum_{m=1}^n a_m u_{mi} \quad m = 1, 2, \dots, n, \quad (1)$$

式中:  $a_m$  为待定常数。把上式代入最小势能方程可求得系统的总势能为

$$\Pi(u_i) \approx \Pi(a_{1i}, a_{2i}, \dots, a_{ni}). \quad (2)$$

再根据式  $\delta \Pi = 0$ , 即得

$$\frac{\partial \Pi}{\partial a_{mi}} = 0 \quad (3)$$

因应变能函数是应变分量的二次齐次式,  $\Pi$  中最高只能含  $a_{mi}$  的二次项, 故上式应为以  $a_{mi}$  为未知量的线性代数方程。

如图 2 所示的简支梁在  $x = c$  处作用一集中力  $P$ ,  $c$  为原点到力的作用点的距离, 可求其挠度曲线。问题的边界条件为  $x = 0, \omega = 0; x = 1, \omega = 0$  故可

取位移  $\omega = \sum_{m=1}^{\infty} a_m \sin \frac{m\pi x}{l}$ , 则系统的应变能为

$$u = \frac{1}{2} EJ \int_0^1 \left( \frac{d^2 \omega}{dx^2} \right)^2 dx = \frac{1}{2} EJ \sum_{m=1}^{\infty} a_m^2 \left( \frac{m\pi}{l} \right)^4$$

$$\mu_1 = \frac{2\rho_{01}(c_{01}^2 + \lambda v_d^2) - \sqrt{[2\rho_{01}(c_{01}^2 + \lambda v_d^2)]^2 - 4\rho_{01}^2 v_d^2 (c_{01}^2 + \lambda v_d^2)}}{2\rho_{01}(c_{01}^2 + \lambda v_d^2)}, \quad (12)$$

式中:  $\lambda_1, \rho_{01}, c_{01}, \lambda_2, \rho_{02}, c_{02}$  分别为基、复板材料常数, 见文献[6, 7]; 对某一特定厚度(密度)的炸药, 爆速  $v_d$  为一定值。

### 2.2 计算实例

以紫铜为复板, 复板厚度 2.8 mm, 低碳钢为基板, 按所研发的计算机系统的计算资料, 采用 2 号岩石炸药, 装药密度  $0.7 \text{ g/cm}^3$  进行爆炸焊接界面基板的应力场模拟计算, 基板低碳钢的泊松比  $\mu = 0.28$ , 弹性模量  $E = 206 \text{ MPa}$ , 抗拉强度  $R_m = 340 \text{ MPa}$ , 塑性变形模量  $[\sigma_p] = 260 \text{ MPa}$ <sup>[5, 6]</sup>, 对不同的炸药速度  $v_d$ , 不同的碰撞角  $\beta$ <sup>[7]</sup> 分四种情况分别进行应力场分布特征模拟计算。

$$\textcircled{1} v_d = 2500 \text{ m/s}, \beta = 12.605^\circ.$$

$$\textcircled{2} v_d = 2800 \text{ m/s}, \beta = 11.459^\circ.$$

$$\textcircled{3} v_d = 3200 \text{ m/s}, \beta = 11.459^\circ.$$

$$\int_0^l \sin \left( \frac{m\pi x}{l} \right) dx = \frac{EJ\pi^4}{4l^3} \sum_{m=1}^{\infty} m^4 a_m^2, \quad (4)$$

式中:  $E$  为材料的弹性模量;  $J$  为截面的惯性矩。

外力势能为

$$\bar{V} = -P \sum_{m=1}^{\infty} a_m \sin \frac{m\pi c}{l}. \quad (5)$$

系统的总势能为

$$\Pi^0 = \frac{EJ\pi^4}{4l^3} \sum_{m=1}^{\infty} m^4 a_m^2 - P \sum_{m=1}^{\infty} a_m \sin \frac{m\pi c}{l}. \quad (6)$$

根据最小势能原理  $\delta \Pi = 0$ , 有

$$\frac{\partial \Pi}{\partial a_m} = 0. \quad (7)$$

$$\text{求得} \quad a_m = \frac{2Pl^3 \sin \frac{m\pi c}{l}}{EJ\pi^4 m^4}. \quad (8)$$

$$\omega = \frac{2Pl^3}{EJ\pi^4} \sum_{m=1}^{\infty} \frac{1}{m^4} \sin \frac{m\pi c}{l} \sin \frac{m\pi x}{l}. \quad (9)$$

上式是挠曲函数的精确解, 若取有限项计算, 即得挠度的近似值。

$$\sigma_z = \frac{E}{2(1-\mu_1^2)} \left[ \frac{h^2}{4} (z - \frac{h}{2}) - \frac{1}{3} (z^3 - \frac{h^3}{8}) \right] \nabla^4 \omega - \frac{Eh^3}{6(1-\mu_1^2)} \left( \frac{1}{2} - \frac{z}{h} \right)^2 \left( 1 + \frac{z}{h} \right) \nabla^4 \omega, \quad (10)$$

式中:  $h$  为竖直位置;  $z$  为板厚;  $\mu_1$  为待定常数。

碰撞压力按下式计算, 即

$$P = \frac{\rho_{01} v_1^2}{2 - \mu_1}, \quad (11)$$

$$\text{式中: } v_1 = \frac{c_{01} \sqrt{\mu_1(2 - \mu_1)}}{1 - \lambda_1 \mu_1};$$

$$\textcircled{4} v_d = 3200 \text{ m/s}, \beta = 12.605^\circ.$$

四种条件焊接面上的应力场分布情况见图 3, 图中水平位置  $x$  表示板的长度方向尺寸, 竖直位置  $y$  表示板的厚度方向的尺寸, 图内数值单位为 MPa。

通过计算及分析, 可以看出以下几方面的规律。

(1) 对于不同的爆炸焊接参数及焊接条件, 可以从图 3 中看出其应力曲线分布和应力的不同, 应力大小不仅与炸药的爆炸速度有关, 而且同时与其主要参数碰撞角  $\beta$  有关。

(2) 碰撞角  $\beta$  的大小是与炸药爆炸速度, 基复板之间的安装间距以及基复板的材料性质有关。因此, 实现可靠的爆炸焊接成品是合理选择以上参数的结果。

(3) 从图 3 中看出, 图 3a, b 中的界面应力已达

到塑性变形强度,但未达到材料的极限抗拉强度,焊接界面将会形成良好的焊接强度。图 3c, d 中的界

面应力已远超过材料的极限抗拉强度,焊接界面将会产生程度不同的过熔现象。

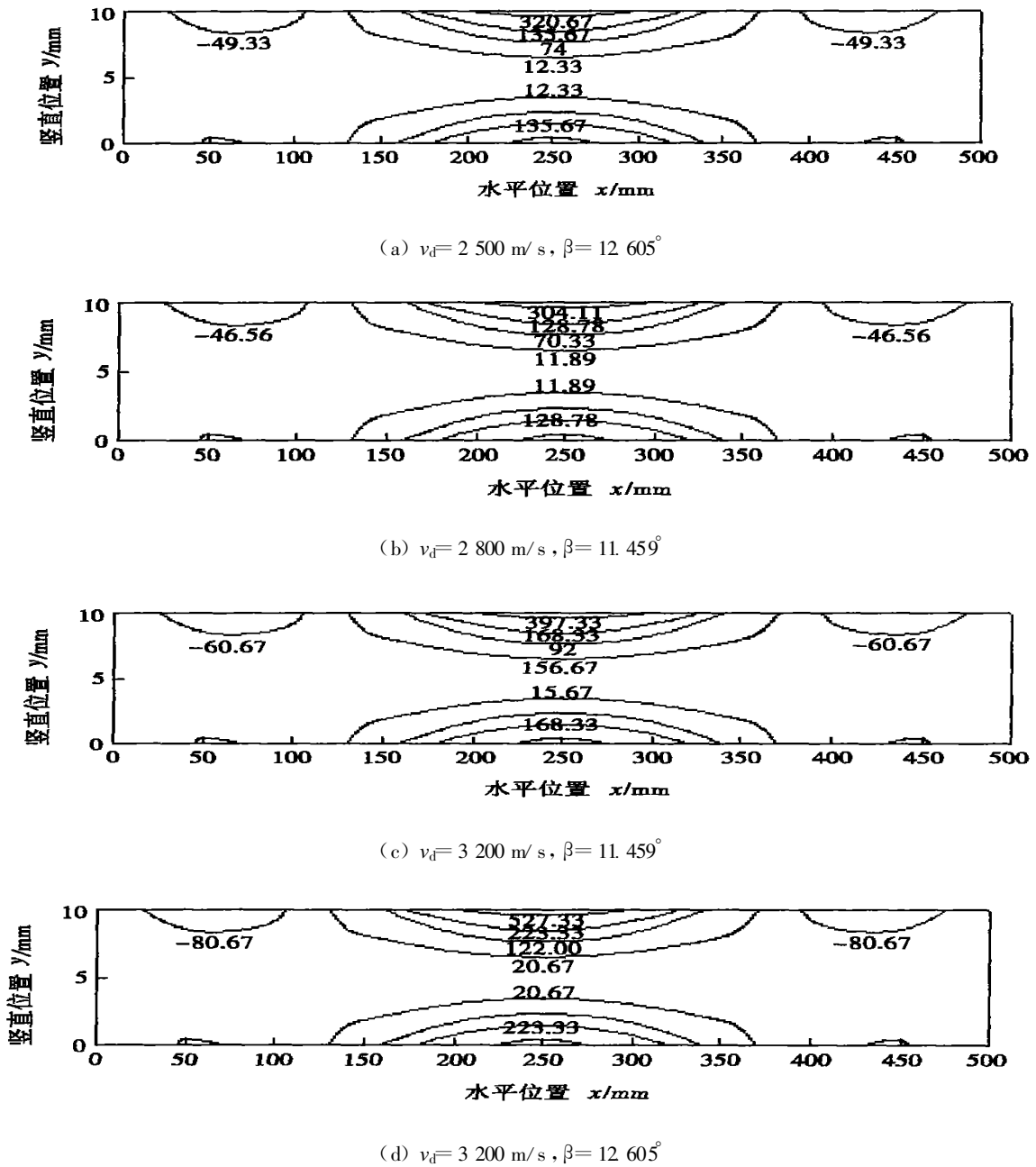


图 3 不同条件下的应力分布情况

Fig. 3 Stress field pattern in different condition

### 3 结 论

复板在炸药爆炸高速冲击力作用下与基板的焊接是一个动态过程,将复板对基板的冲击简化为碰撞点作用的简支模型,并采用瑞利—里兹法计算模型,以紫铜为复板,低碳钢为基板,并分别针对不同的炸药及基复板安装条件计算出碰撞点的应力及分

布情况。由碰撞应力所形成的基板的应力场计算结果可以看出,在选用常用的 2 号岩石硝铵炸药、基复板材料性质、尺寸确定的情况下,金属爆炸焊接试件的焊接质量,主要依赖于炸药的敷设厚度、复板对碰撞角等参数,对爆炸应力场在基板中的分布给出了定性、定量的描述,对金属爆炸焊接工程具有一定的指导作用。

[下转第 93 页]

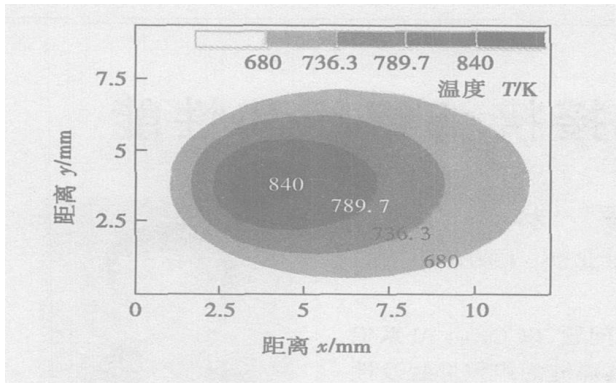


图 8 数值模拟背面温度场

Fig. 8 Back temperature field of numerical simulation

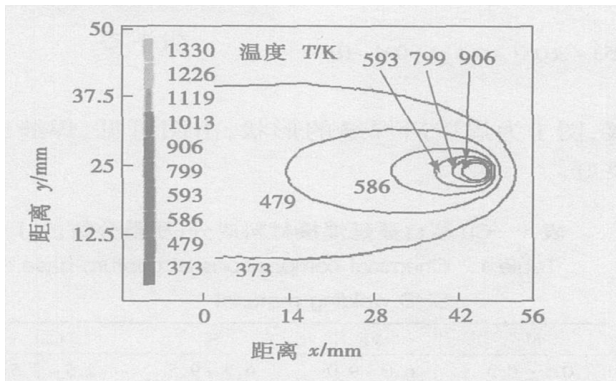


图 9 数值模拟正面温度场

Fig. 9 Front temperature field of numerical simulation

## 5 结 论

(1) 提出一种基于红外辐射测温原理并针对红外热像仪的焊接温度场测量与校正方法。实温校正方法可准确校正试件表面一致区域的温度场, 表面校正方法可消除焊缝表面变化而引起的对温度场分布的影响。

(2) 通过结合应用实温校正和表面校正方法能准确地校正镁合金激光-TIG 复合热源焊接过程中电弧覆盖范围外的温度场。

(3) 焊接温度场数值模拟可以比较准确预测并反映实际温度场的分布, 弥补电弧覆盖区域的温度场缺失, 最终获得整体的镁合金激光-TIG 复合热源焊接温度场分布。

## 参考文献:

- [1] 拉达伊 D. 焊接热效应[M]. 北京: 机械工业出版社, 1997
- [2] 吴继宗, 叶关荣. 光辐射测量[M]. 北京: 机械工业出版社, 1989.
- [3] 西格尔 R, 豪厄尔 J R. 热辐射传热[M]. 北京: 科学出版社, 1990.
- [4] 侯成刚, 张广明, 赵明涛, 等. 用红外热像仪技术精确测定物体发射率[J]. 红外与毫米波学报, 1997, 16(3): 193-198
- [5] 杨立, 寇蔚, 刘慧开, 等. 热像仪测量物体表面辐射率及误差分析[J]. 激光与红外, 2002, 32(1): 43-45.
- [6] Farson D, Richardson R, Li X. Infrared measurement of base metal temperature in gas tungsten arc welding [J]. Welding Research Supplement, 1998(3): 96-401.
- [7] 潘际奎. 现代弧焊控制[M]. 北京: 机械工业出版社, 2000
- [8] 吴雷, 赵海燕, 王煜, 等. 高能束焊接数值模拟中的新型热源模型[J]. 焊接学报, 2004, 25(1): 92-94.
- [9] Chong L M. Predicting welding hardness [D]. M. Eng. Thesis. Ottawa Canada; Carleton University, 1982.
- [10] 刘黎明, 迟鸣声, 宋刚, 等. 镁合金激光-TIG 复合热源焊接热源模型的建立及其数值模拟[J]. 机械工程学报, 2006, 42(2): 82-86.

**作者简介:** 黄瑞生, 男, 1981年1月出生, 博士研究生。主要从事激光-电弧复合热源焊接及焊接温度场分析等方面的研究。已发表论文2篇。

Email: liuh@dlht.edu.cn

[ 上接第 28 页 ]

## 参考文献

- [1] 郑哲敏, 杨振声. 爆炸加工[M]. 北京: 国防工业出版社, 1981.
- [2] 邵丙璜. 炸药在滑移爆轰作用下多方指数值的确定[J]. 爆炸与冲击, 1981, 1(2): 30-36.
- [3] 邵丙璜, 张凯. 爆炸焊接原理及其应用[M]. 大连: 大连工学院出版社, 1987.
- [4] 王子昆, 黄上恒. 弹性力学[M]. 西安: 西安交通大学出版社, 1995.

- [5] YihHsing Pao, ChaoChow Mow. Diffraction of elastic and dynamic stress concentrations crane[M]. in US Russak & Compay Inc. 1937.
- [6] Grossland B. Explosive Welding of Metals and Its application[M]. Oxford; Clarendon, 1982
- [7] 谢飞鸿, 关惠平, 王军, 等. 爆炸焊接有效多方指数及可焊窗口研究[J]. 焊接学报, 2004, 25(4): 35-38.

**作者简介:** 谢飞鸿, 男, 1965年10月出生, 副教授。主要从事岩土力学、爆炸力学和复合材料力学研究和教学工作。发表论文26篇

Email: exbeen@126.com

pass welding with large current (DS) was put forward. The experimental results show the tensile strength of the DS joint is up to 296.4 MPa, equivalent to 61.2% of that of base metal and the impact toughness of the DS joint improved simultaneously. The DS weld zone is composed of  $\alpha$  phase and eutectic structure grains. Hardness of the weld is the lowest on the whole weldment, and the hardness of the HAZ is higher because the  $\theta$  phase dissolve and separate out renewedly.

**Key words:** 2519 high strength aluminum alloy; tandem gas metal arc welding; procedure

#### **Numerical simulation on fracture mechanics parameters of welded joint with damage**

ZHANG Jian-xun, LI Ji-hong (State Key Laboratory for Mechanical Behavior of Materials, Xi'an Jiaotong University, Xi'an 710049, China). p19-22

**Abstract:** The fracture mechanics parameters of welded joint with damage were numerically simulated with fully coupled strain and damage elastic-plastic finite element method for center-cracked specimens with welded joint. The results show that the rupture strain of base metal has large effects on the fracture behavior of crack in weld metal. If mechanical parameters of weld metal are kept constant, the plastic strain along the ligament and the J-integral increase with the decrease of the rupture strain of base metal for any strength matching ratio. With the decrease of strength matching ratio (viz. the increasing of the strength of base metal), the effect of the rupture strain of base metal on the J-integral is weakened gradually.

**Key words:** damage; welded joint; fracture mechanics parameters; finite element method

#### **Discussion on determination of J-integral and comparison of different test standards**

DENG Cai-yan, ZHANG Yu-feng, HUO Li-xing (School of Materials Science and Engineering, Tianjin University, Tianjin 300072, China). p23-25, 32

**Abstract:** According to different fracture toughness test standard, J-Resistance curve tests were conducted at  $-5^{\circ}\text{C}$  in welded joints of X56 pipeline steel in the multiple specimen method and the test result were compared. According to the double P-V curves of each weld metal and heat affected zone specimen obtained from the two notch opening displacement, the load-line displacement and the value of J were calculated. Finally, the best fitted curve was determined the valid data points according to GB2038-91 and BS7448, respectively. The result indicates that BS7448 is superior to GB2038-91 on blunt line, exclusion lines and so on. J-Resistance curves and  $J_{0.2}$  was obtained. But there are no valid data points according to GB2038-91 and no further calculation.

**Key words:** J integral; resistance curve; blunt line

#### **A numerical calculation on contact surface stress field of metals explosive welding**

XIE Fei-hong<sup>1,2</sup>, LUO Guan-wei<sup>3</sup>, WANG Xu-guang<sup>4</sup> (1. School of Civil Engineering, Lanzhou Jiaotong University, Lanzhou 730070, China; 2. School of Civil and Environmental Engineering, Beijing University of Science and Technology, Beijing 100083, China; 3. College of Mechanical-Electronics Engineer-

ing, Lanzhou Jiaotong University, Lanzhou 730070, China; 4. Beijing General Research Institute of Mining and Metallurgy, Beijing 100044, China). p26-28, 93

**Abstract:** The impact pressure produced by explosive detonation is essential condition of the base plate and cladding plate coalescence for metal explosion welding. Based on Rayleigh-Ritz calculating model and elasticity variation principle, elasticity problem is considered as functional arrest ental equation, and boundary condition of the problem is given. Differential equation and corresponding boundary condition are derived. Instantaneous stress field at impact points was calculated, and analog calculating of different collision angles and impact pressures were carried out. Basic law of stress field distribution at impact points was found. The calculating stress field distribution law can be applied to evaluation and guidance of practical engineering.

**Key words:** explosive welding; calculation model; impact pressure; stress field; value calculation

#### **Agglomerated alkali flux for submerged arc welding of high strength-toughness steel X80**

ZHANG Min, YAO Cheng-wu, LIU Bin, LI Ji-hong (School of Material Science and Engineering, Xi'an University of Technology, Xi'an 710048, China). p29-32

**Abstract:** Through analyzing acicular ferrite nucleating mechanism in the weld metal of the high strength low-alloy structural steel (HSLA), a submerged arc welding agglomerated flux with the  $\text{CaF}_2\text{-MgO-Al}_2\text{O}_3\text{-MnO-TiO}_2\text{-B}_2\text{O}_3$  fluorine was developed by using alkali flux system. The results indicate that the existence of MnO in the flux benefits the transition of Mn to weld metal, and brings down the  $\gamma \rightarrow \alpha$  transformation temperature, thus high temperature ferrite production is held down, but the acicular ferrite increases in the weld metal. Because the  $P_{cm}$  of weld metal is higher, the austenite grain is thinner as welded in air cooling condition. However, a excessive content of MnO in the flux will lead to the excessive Mn in the weld metal and a too low  $\gamma \rightarrow \alpha$  transform temperature. Thereby, the austenite grain boundaries cannot be decorated by allotriomorphic ferrite, thus the austenite grain boundary increases, which make more bainite nucleation site being produced. It is disadvantageous to the intragranularly nucleated acicular ferrite. In addition, the rare-earth element has some contributions to enhance the acicular ferrite content in the weld metal.

**Key words:** agglomerated flux; strength and toughness; acicular ferrite; intragranular nucleation; phase transformation temperature

#### **CO<sub>2</sub> laser welding process of aluminum alloy with filler powder**

CHEN Kai, XIAO Rong-shi, ZHANG Seng-hai, ZUO Tie-chuan (College of Laser Engineering, National Center of Laser Technology, Beijing University of Technology, Beijing 100022, China). p33-36

**Abstract:** The experiments were carried out with CO<sub>2</sub> (slab) laser. The five stages of the inter actions between laser and powder in the laser welding with powder were analyzed. The influences of the filler metal powder on the laser power density threshold value, weld formation and process stability were studied during CO<sub>2</sub> laser